

Methods

Animal husbandry and mouse models. Mice were housed in pathogen-free conditions in an American Association for the Accreditation of Laboratory Animal Care-approved facility managed by the Department of Animal Resources of Emory University. All animal studies were approved by the Institutional Animal Care and Use Committee (IACUC) of Emory University, and performed in accordance with IACUC guidelines and regulations. We confirm that all experiments were performed in accordance with IACUC guidelines and regulations. C57BL/6 wild type (Jackson Laboratory, 000664) male and female mice were used for breeding and for the studies reported here. Animal husbandry was performed as described^{10,11}. For cardiomyocyte lineage tracing studies, we used *Rosa26fs-Confetti* [B6.129P2-Gt(ROSA)26Sortm1(CAG-Brainbow2.1)Cle/J, Jackson Laboratory, 017492] and *Myh6-MerCreMer* [B6.FVB(129)-A1cfTg(*Myh6-cre*/Esr1*)1Jmk/J, Jackson Laboratory, 005657] mice. We then generated double-transgenic *Myh6-MerCreMer::Rosa26fs-Confetti* mice by cross breeding. In the double transgenic mice, Cre recombinase causes the Brainbow 2.1 construct to recombine, which randomly labels cardiomyocytes either with GFP, CFP, RFP or YFP. We limited the extent of Cre-mediated recombination by adjusting the dose of 4-hydroxytamoxifen (H7904-5mg, Sigma) to minimize replication-independent occurrences of adjacent cardiomyocytes of the same color.

Drugs such as T3, danusertib and 4-hydroxytamoxifen were administered, intraperitoneally (i.p.), to each mouse at the dose indicated. Vehicle was administered by the same route and animals thus treated served as controls. Phosphate buffered saline (PBS) was the vehicle for T3, 50% DMSO in PBS for danusertib, and soybean oil for 4-hydroxytamoxifen. DUSP5-specific siRNA or scrambled siRNA (control) was administered using *in vivo*-jetPEI®, (VWR, 89129-960). DUSP5 siRNA (100 µg) was dissolved in 1 ml of the *in vivo*-jetPEI:10% glucose mixture and was injected 100 µl per mouse i.p. (10 µg/mouse). DUSP5 siRNA (sc-60555) was a pool of 2 different siRNA duplexes (sc-60555A, sense: CAUGGCUUACCUCAUGAA and antisense: UUCAUGAGGUAAGCCAUGCtt; sc-60555B, sense: GACAGCUCCUUCAGUAUGA and antisense: UCAUACUGAAGGAGCUGUCtt; Santa Cruz Biotechnology). All sequences are provided in 5'→3' orientation. We did not use any litters if one or more mouse in the litter was observed to be sick. Mice were first anesthetized with 5% isoflurane and then hearts harvested for further processing. Hearts were also collected at 40 h after T3 or vehicle treatment and ventricular cardiomyocytes prepared for immunoblotting or immunocytochemistry. In addition, hearts were collected post-therapy for immunocytochemistry, immunohistochemistry and cardiomyocyte number determination.

Echocardiography analysis. Transthoracic echocardiography was performed as described¹¹. Briefly, echocardiography was performed under light isoflurane anesthesia on either DUSP5 siRNA or scrambled siRNA ± T3 treated mice using the Vevo 3100 imaging platform (VisualSonics Inc.) with a MX550D linear array transducer (axial resolution: 40 µm) and images were analyzed using Vevo® Lab Desktop Software. Both B-mode and M-mode images were collected to assess cardiac morphology and function. Parasternal short axis M-mode echocardiographic imaging was used to determine wall thicknesses and internal diameter of the LV at diastole and systole; fractional shortening was derived from these parameters. The intraventricular septum (IVS) function of M-mode (short axis) of Vevo® Lab Desktop Software was used to determine these parameters. Endocardium and epicardium were outlined using the IVS function by tracing the anterior epicardial, endocardial and then posterior endocardial and epicardial wall. These measurements were made at the mid-apical level (half-way between the

apex and the LV mid papillary level; ~1 mm from the apex) or mid-papillary level (~3.5 mm from the apex). Additionally, B-mode parasternal long axis images were acquired to determine LV long axis internal diameters and wall thicknesses. Using B-mode (long axis), the length of the LV chamber was determined by measuring the distance from the aortic root to the apical endocardial wall at end-systole and end-diastole. We also measured LVPW thickness at the apex using B-mode (long-axis) by tracing the apical wall from the epicardium to endocardium. LV volumes at end-diastole and end-measurements were calculated using the LV-trace function of the Vevo® Lab Desktop Software in B-mode. LV endocardial borders were traced at end-diastole and end-systole by tracing the aortic root, apex, anterior wall, posterior wall and retracing the anterior and posterior wall until the myocardial wall is outlined. The Vevo® Lab Desktop Software automatically determines volumes at end-diastole, end-systole, and calculates LV volume, SV and LV ejection fraction. At least three different images were taken for each cardiac parameter and measurements from these three individual images were averaged to acquire final measurement for that cardiac parameter.

Cardiomyocyte number determination. The protocol for cardiomyocyte number determination was as described previously^{10, 11}. Briefly, heparin (100–200 µl, 1000 USP units/ml) was injected intraperitoneally eight minutes prior to harvesting. Hearts were harvested under deep anesthesia (5% isoflurane). Hearts with their atria and aorta attached were washed with PBS and then the aorta cannulated for retrograde perfusion through the coronary circulation. Hearts were immediately perfused with Cytifix (BD Biosciences, 554655) for 1 min. Subsequently, hearts were perfused with perfusion buffer (120 mM NaCl, 15 mM KCl, 0.5 mM KH₂PO₄, 5 mM NaHCO₃, 10 mM HEPES, and 5 mM glucose, at pH 7.0) for 2 min and then with perfusion buffer containing collagenase type 2 (Worthington, LS004176) for 10–15 min at 37 °C. Perfusion and digestion buffers were freshly prepared, warmed to 37 °C and aerated with 5% CO₂. Collagenase concentration was 2 mg/ml. After ~12 min of digestion, the atria were excised and the cardiac ventricles placed in a 6 cm dish containing 2 ml of digestion buffer; we then added ~2 ml of STOP buffer (perfusion buffer plus 10% bovine calf serum and 12.5 mM CaCl₂). The ventricles were teased apart into small pieces followed by trituration through pipettes of progressively smaller diameters. The digested cardiomyocytes from each heart were collected in a 15 ml falcon tube and more STOP buffer was added to a volume of 10 ml. The final cell suspension was used to count cardiomyocytes using a hemocytometer. To avoid losses, cardiomyocytes were not purified, but could be readily identified by phase contrast microscopy based on their cytoplasmic size and rod shape. Four aliquots were counted per heart and the mean value was used to determine the total number of ventricular cardiomyocytes per heart.

For accurate cardiomyocyte number determination, a critical step is optimal digestion efficiency and operator-specific variability in isolation and counting. We have eliminated operator-specific variability by using the same operator between experiments. Heart digestion is chiefly dependent on collagenase concentration in the perfusion medium, its activity, exposure time and temperature. To optimize digestion efficiencies, these variables were adjusted for each group of mice depending on the age of the mouse. Importantly, collagenase activity was kept uniform between the biological replicates and across experiments by using the same lot of enzyme. Additionally, a brief fixation with Cytifix (~1 min) before starting perfusion with collagenase was used to maintain cardiomyocyte structure and to prevent the generation of fragmented cardiomyocytes. Cardiomyocytes during the postnatal stages analyzed are much larger than non-myocytes and are readily identifiable due to their cytoplasmic size and rod-

shape¹⁰. Digestion efficiency was calculated [ventricular weight %, determined by (original weight – residual)/original weight] after each change in condition. We found that maximal digestion efficiencies were between ~ 97% and 99%. Upon microscopic examination, the residual tissue was almost entirely undigested cardiac valves and blood vessels. Over-digestion neither improved digestion efficiencies, nor did it increase cardiomyocyte yield. We did not estimate cardiomyocyte numbers from under-digested hearts in which disaggregation of myocardial tissue was incomplete. Suboptimal cannulation of the aorta was the cause of under-digestion but was infrequent.

Cardiomyocyte isolation for immunocytochemistry and immunoblotting. For immunoblotting and immunocytochemistry, hearts were enzymatically digested as described above. Before making single cell suspensions, atria were excised, and the LVs were trimmed from the RV. Cardiomyocytes were purified with three low speed centrifugations (18 x g for 4 min at room temperature), which caused cardiomyocytes to settle as a pellet. Supernatant fractions, enriched in non-myocytes, were discarded. Resulting cardiomyocyte preparations were > 95% pure. Aliquots of cardiomyocytes were snap frozen in liquid nitrogen and stored at –80°C for immunoblotting. Additionally, aliquots were fixed with Cytfix (BD Biosciences, 554655) for 5 min and spread on glass slides for immunocytochemistry.

Immunofluorescence. Immunofluorescence was performed as described earlier^{10,11}. Briefly, cardiomyocytes were isolated as described above and fixed in Cytfix (BD Biosciences, 554655) for 5 min. After pre-blocking, cardiomyocytes were stained with anti-cardiac troponin T- (Miltenyi Biotec, 130-119-674), in 10% v/v goat serum. DAPI was used to stain nuclei. High power (40X) images were acquired on a Leica Microsystems DMZ6000 microscope by using the LAX program and analyzed using Nikon's NIS Elements advanced fluorescence program, to determine cardiomyocyte size.

Immunohistochemistry. Mouse hearts were immersion-fixed in 10% formalin and then stored in 70% ethanol until paraffin embedding and sectioning. Paraffin-embedded sections (~7 µm) were mounted on ++ glass slides and were deparaffinized with xylene and then rehydrated in ethanol. Antigen retrieval was performed using sodium citrate buffer. The mounted sections, immersed in sodium citrate buffer, were boiled for 3 minutes using a microwave oven. Sections were blocked with 10% v/v goat serum for 30 min at room temperature before applying primary antibody: wheat germ agglutinin ((WGA)-Alexafluor 647 conjugate (W32466, ThermoFisher) to identify cell borders. After a 60 min incubation at room temperature sections were washed three times for five minutes each with PBS, and then coverslips were mounted using mounting media containing DAPI (4',6-diamidino-2-phenylindole) to identify nuclei. High power (63X) images were acquired on a Leica Microsystems DMZ6000 microscope using the LAX program and analyzed using Nikon's NIS Elements advanced fluorescence program.

Histology. Heart sections, prepared and processed as described above, were stained using a trichrome stain kit (ab150686, Abcam) as per manufacturer's protocol. Images were acquired and processed using Hamamatsu's NanoZoomer-SQ Digital slide scanner and NDP.view2 Viewing software.

Immunoblotting. The protocol used was as described previously^{10,11}. Whole cell cardiomyocyte

lysates were generated by re-suspending cardiomyocytes in 250 μ l of RIPA buffer (Cell Signaling, 9806S) supplemented with phosphatase inhibitor cocktail 2 and 3 (Sigma-Aldrich, P5726-1ML and P0044-1ML), 0.1 mM phenylmethylsulfonyl fluoride (PMSF, Sigma-Aldrich, 93482-50ML-F) and protease inhibitor cocktail (Roche, 11697498001). Cardiomyocytes were lysed by sonication and then pelleted by centrifuged at 21,000 x g for 30 min. The resulting supernatant fractions were aliquoted into fresh Eppendorf tubes and then snap-frozen in liquid nitrogen. Aliquots stored at -80 $^{\circ}$ C, were allowed to thaw on ice immediately before use. Initially, a 5 to 10 μ l aliquot (\sim 20 μ g protein) was mixed with an equal volume of 2x Laemmli sample buffer (Bio-Rad, 1610737), heated for 5 min at 95–99 $^{\circ}$ C and then immediately cooled on ice for 5 min. The samples were then centrifuged briefly before loading onto and fractionation by SDS–polyacrylamide gel (12–18%) electrophoresis (SDS-PAGE), which was performed at 200 volts for 5 min, and then at 150 volts for 30 min to 2 h. Proteins thus resolved were then transferred to a PVDF membrane by electroblotting (Turbo Transfer; Bio-Rad). Depending upon the molecular weight of the proteins or protein complexes, the transfer time was varied for high (11 min), medium (7 min) and low (5 min) molecular weight proteins. After transfer, all blots were pre-blocked for 30–60 min in Superblock (Thermo Scientific, 37536). Initially, the samples were probed with GAPDH antibody. Based on GAPDH, loading of each sample was adjusted so that all samples contained an equal amount of GAPDH. Membranes were probed with the target protein-specific primary antibody. For quantitative analysis, the membrane was then stripped and re-probed with GAPDH to ensure that loading was normalize for each sample. For stripping, the membrane was washed twice with 1x Tris-buffered saline (TBS, Thermo Scientific, BP2471-1) for 5 min each and then incubated with Restore™ Western Blot Stripping Buffer (Thermo Scientific, 21059) for 5–15 min and then washed again twice with 1x TBS and pre-blocked with Superblock (37536, Thermo Scientific) for 1 h before incubating with GAPDH antibody. Primary antibodies (see below) were also diluted in Superblock and incubated for 2 h at 22 $^{\circ}$ C, or overnight at 4 $^{\circ}$ C, followed by horseradish peroxidase (HRP)-labeled secondary antibody (1:10,000) for 45 min at 22 $^{\circ}$ C. The signals were detected using Super Signal West Dura Detection Reagent (Thermo Scientific, 34075) and images captured on a Bio-Rad GelDoc system equipped with CCD camera and ImageLab program (Bio-Rad). Quantification was performed by densitometry using the ImageLab program. Antibodies used for immunoblots are DUSP5 (ab200708, Abcam), ERK1/2 (4695, Cell Signaling), p-ERK1/2 (4370, Cell Signaling), cyclin D1 (ab134175, Abcam) and GAPDH (2118, Cell Signaling). Most of these antibodies are profiled in 1DegreeBio and were additionally validated using siRNA knockdown.

Statistical analysis. Statistical significance of data was determined using Graphpad Prism 8. The Shapiro-Wilk test was used to determine if the data were normally distributed; in this case, we used one-way ANOVA followed by Sidak multiple comparisons test, or unpaired two-tailed Student's *t*-test for comparisons involving 2 groups. For estimation of variance, the F-test was used when comparing 2 groups and the Brown-Forsythe test was used when comparing multiple groups by 1-way ANOVA. *P*-values < 0.05 were considered significant. Results are expressed as mean \pm s.e.m. This study did not involve Bayesian analysis, information on the choice of priors and Markov chain Monte Carlo settings. This study also did not require hierarchical and complex designs, identification of the appropriate level for tests and full reporting of outcomes. Estimates of effect sizes were also not utilized in this study.

Reporting Summary. Further information on research design is available in the Nature

Research Reporting Summary linked to this article.

Data availability

The data and resources generated for this manuscript are available upon reasonable request from the corresponding authors.

Code availability

This study does not utilize a custom code or mathematical algorithm to generate data.

Acknowledgements

This work was supported by grants from the Department of Medicine, Emory University, the Carlyle Fraser Heart Center, Emory University Hospital Midtown, the NIH (HL079040, HL127726, HL098481, T32HL007745, HL092141, HL093579, HL094373 and HL113452), the American Heart Association (13SDG16460006; 17GRNT33670975), the Fondation Leducq Transatlantic Network, National Health and Medical Research Council, Australia (APP1074386), R.T. Hall estate, the Australian Research Council Stem Cells Australia and Special Initiative in Stem Cell Science grant (SR1101002).

Author contributions

A.H. and N.N were responsible for the original concept and design of primary experiments. L.T. performed western blotting, drugs administration and tissue harvesting. N.B. performed echocardiography to acquire images for L.T. to analyze, determined cardiomyocyte number and also isolated cardiomyocytes for western blotting. L.T analyzed echocardiography images. E.N. determined cardiomyocyte and capillary densities. J.W.C. assisted N.N. in performing immunohistochemical studies. A.H., N.N., R.M.G., and R.W.T. prepared the manuscript. All authors discussed the results and edited the manuscript.

Competing Interests

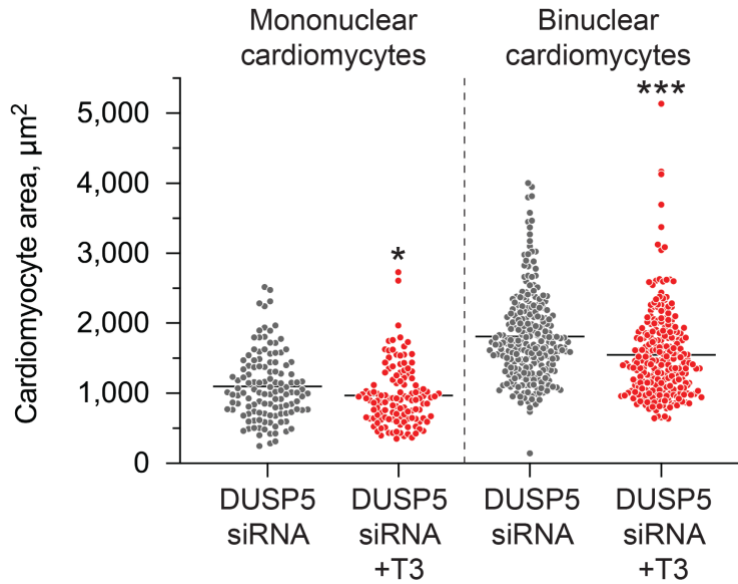
The authors declare no competing interests.

Additional information

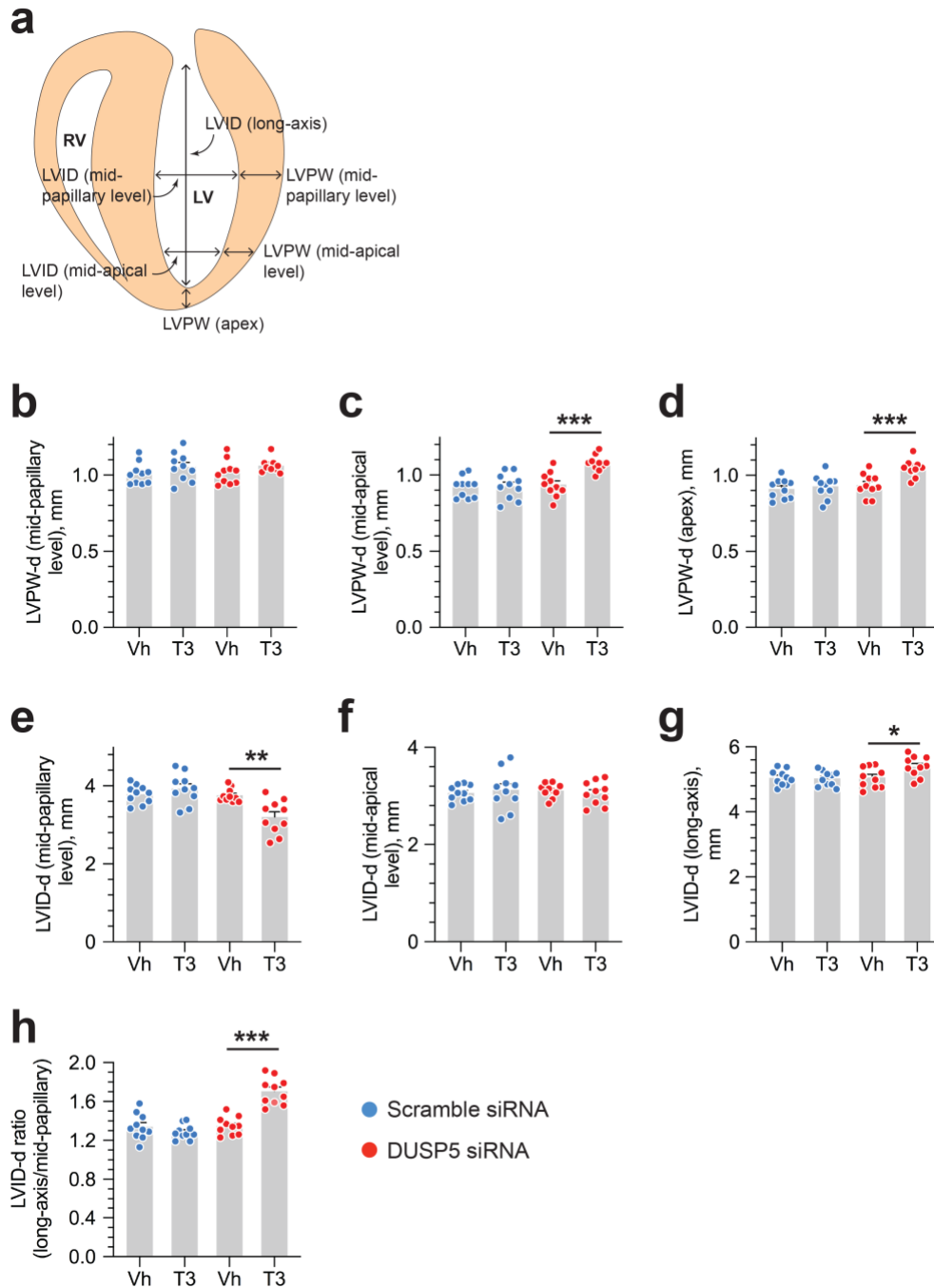
Extended data includes 7 Figures and 2 Videos and is available online.

Supplementary information includes detailed Methods and is available online.

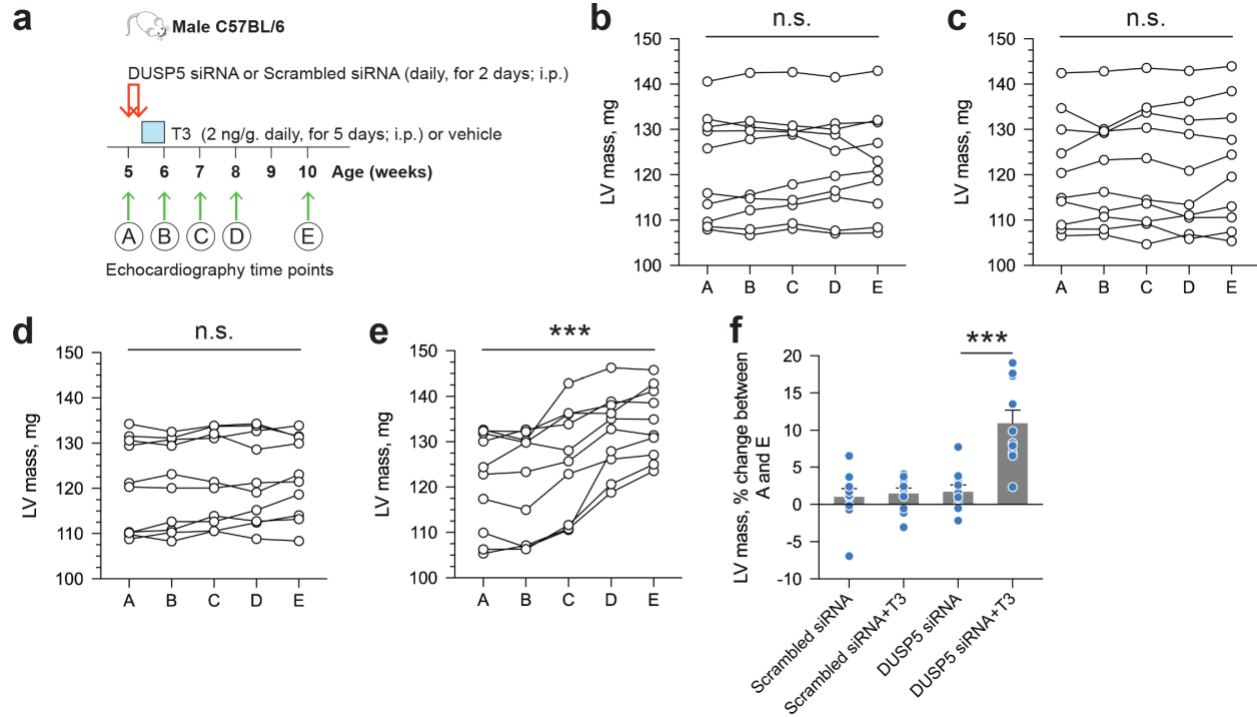
Correspondence and requests for materials should be addressed to A.H. or N.N.



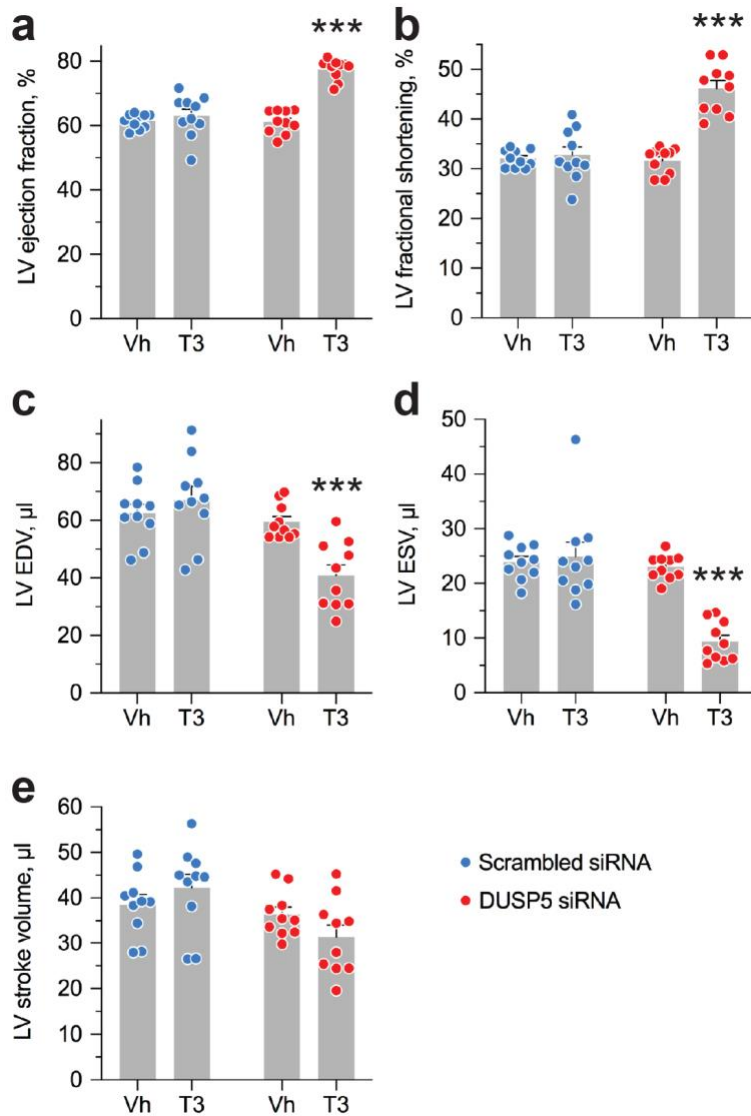
Extended Data Fig. 1 | DUSP5 siRNA+T3 therapy in young adult (5-week-old) mice results in a decrease in average ventricular cardiomyocyte size. Mono-nuclear (left) and binuclear cardiomyocyte (right) areas were smaller 4-weeks after DUSP5 siRNA+T3 therapy than after DUSP5 siRNA monotherapy. Ventricular cardiomyocyte areas were evaluated using Nikon NIS-Elements software; cardiomyocytes, in cell smears, were identified using cardiac troponin T-staining and nucleation state of the cell was determined by 4',6-diamidino-2-phenylindole (DAPI) staining ($n = 200$ binuclear and 100 mononuclear cardiomyocytes pooled from the analysis of 4 mice per therapy group). Bars represent mean values. Comparison between groups was made using a 2-tailed t -test. $*P < 0.05$, $***P < 0.001$.



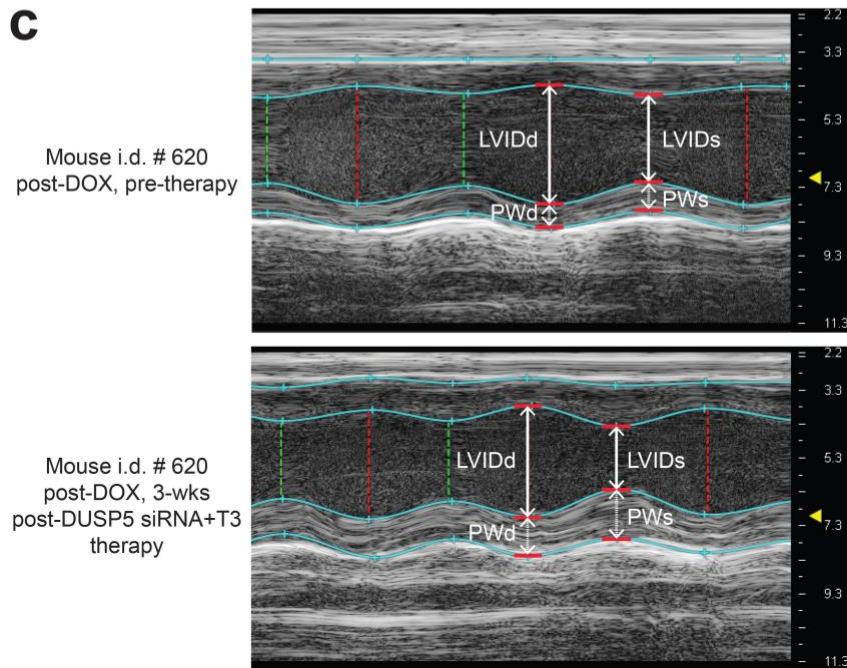
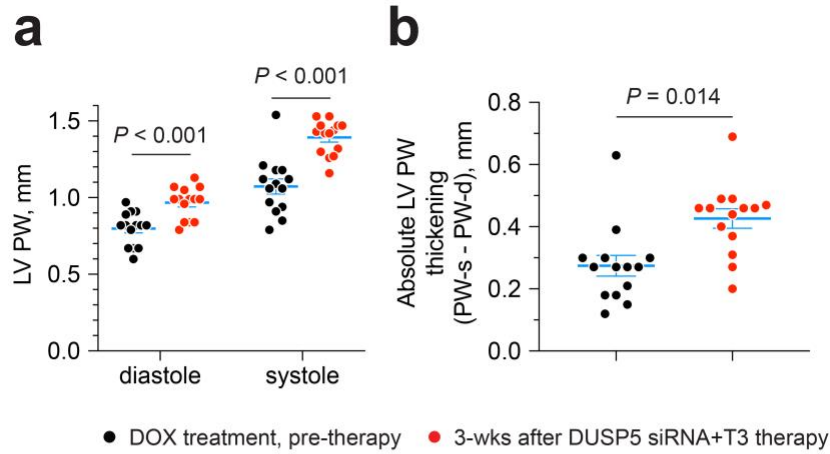
Extended Data Fig. 2 | DUSP5 siRNA+T3 therapy induces LV growth and LV chamber elongation in young adult (5-week-old) mice. **a**, Diagram showing sites of LV dimension measurements using echocardiography. **b–g**, Effect of T3 therapy in mice pretreated with either DUSP5 siRNA or scrambled siRNA (control) on posterior wall (PW) dimensions at diastole at the LV mid-papillary (**b**) and mid-apical level (**c**) and at the LV apex (**d**), and LV chamber internal dimensions (LVID) at diastole at the LV mid-papillary (**e**) and mid-apical level (**f**) and LVID long axis (**g**). **h**, LVID long-axis-to-mid-papillary ratio at diastole ($n = 10$ mice per group); * $P < 0.05$, ** $P < 0.01$, *** $P < 0.001$. Mean \pm s.e.m. Comparisons were made using ANOVA with Sidak multiple comparison test; only within group P -values are shown.



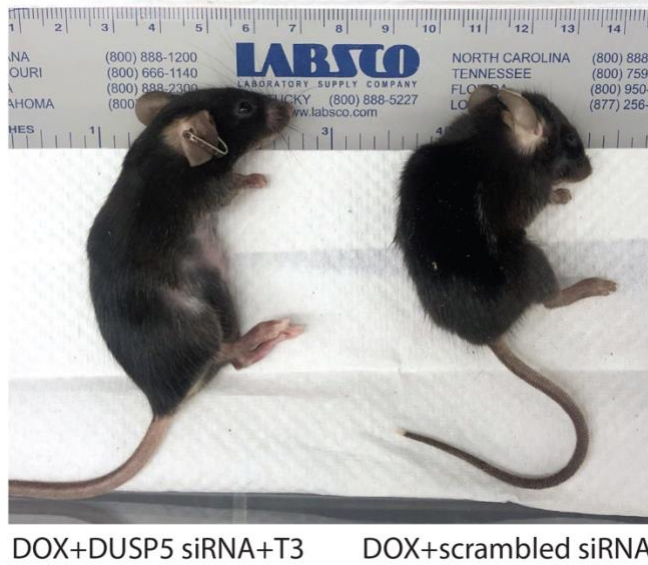
Extended Data Fig. 3 | LV mass increases progressively, but after the cessation of DUSP5 siRNA+T3 therapy, in young adult (5-week-old) mice. **a**, Diagram showing the time points before and after DUSP5 siRNA+T3 therapy at which LV mass was determined using echocardiography. Serial determinations of LV mass before and after therapy with scrambled siRNA (control) (**b**), scrambled siRNA+T3 (**c**), DUSP5 siRNA (**d**) and DUSP5 siRNA+T3 (**e**) ($n = 10$ mice per group). Comparisons were made using a paired 2-tailed t -test between time points A and E. *** $P < 0.001$. **f**, Relative change (%) in LV mass between the start of therapy and 4-week after therapy ($n = 10$ pairs per group). Comparisons were made using ANOVA with Sidak multiple comparison test; only within group P -values are shown. Mean \pm s.e.m. *** $P < 0.001$.



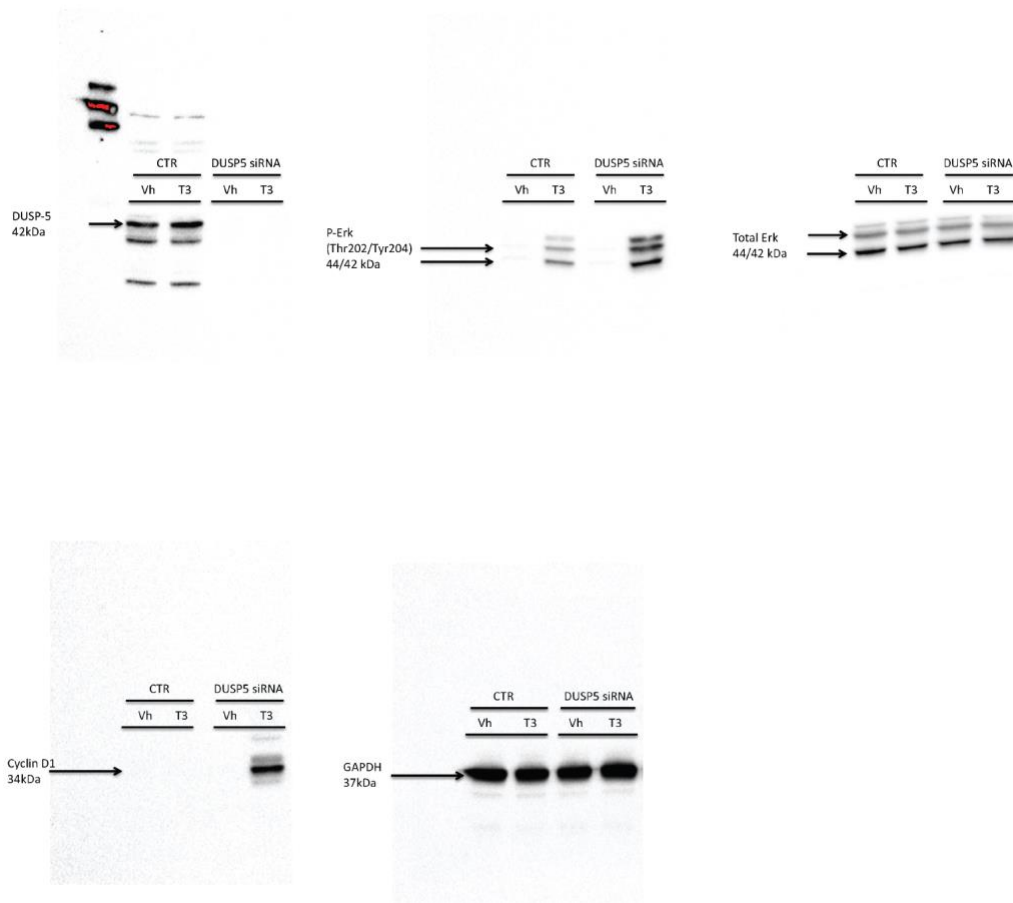
Extended Data Fig. 4 | DUSP5 siRNA+T3 therapy potentiates LV contractile function in young adult (5-week-old) mice. a–e, Effect of T3 therapy in mice pretreated with either DUSP5 siRNA or scrambled siRNA (control) on LV ejection fraction (a), LV fractional shortening (b), LV end-diastolic volume (EDV) (c), LV end-systolic volume (ESV) (d) and LV stroke volume (e) ($n = 10$ mice per group). Mean \pm s.e.m. Comparisons were made using ANOVA with Sidak multiple comparison test; only within group P -values are shown. *** $P < 0.001$.



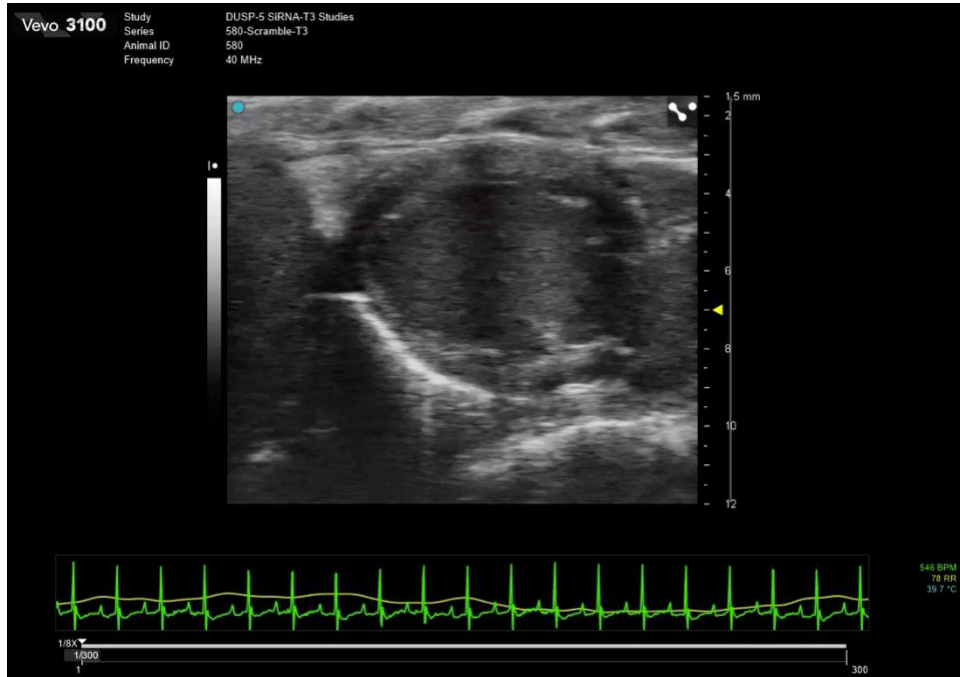
Extended Data Fig. 5 | DUSP5 siRNA+T3 therapy potentiates contractile function at the LV mid-papillary level in mice with doxorubicin cardiomyopathy. a,b, LV posterior wall (PW) dimensions at diastole and systole (a), and absolute LV PW thickening at systole (b), before and 3 weeks after DUSP5 siRNA+T3 therapy in doxorubicin-injured hearts ($n = 14$ mice per group). Comparisons were made using a 2-tailed t -test. Mean \pm s.e.m. c, Representative M-mode images of a mouse heart before and after DUSP5 siRNA+T3 therapy. LV internal dimensions at diastole (LVIDd) and systole (LVIDs) as well as PW dimensions at diastole (PWd) and systole (PWs) are indicated.



Extended Data Fig. 6 | Representative images of mice with doxorubicin cardiomyopathy 3 weeks after DUSP5 siRNA+T3 or scrambled siRNA (control) therapy. After scrambled siRNA (right), but not DUSP5 siRNA+T3 therapy (left) mice adopt a hunch-back posture and smaller as shown in these representative images.



Extended Data Fig. 7. Uncropped images of immunoblots displayed in Fig. 1a.



Extended Data Video 1. Representative video showing LV trace of parasternal long-axis B-mode image of a young adult mouse heart between full diastole and full systole after therapy with scrambled siRNA+T3.



Extended Data Video 2. Representative video showing LV trace of parasternal long-axis B-mode image of a young adult mouse heart between full diastole and full systole after therapy with DUSP5 siRNA+T3.